Original Article

Integrating shear wave elastography and estimated glomerular filtration rate to enhance diagnostic strategy for renal fibrosis assessment in chronic kidney disease

Ziman Chen[1], Yingli Wang[2], Simon Takadiyi Gunda[1], Xinyang Han[1], Zhongzhen Su[3], Michael Tin Cheung Ying[1]

[1]Department of Health Technology and Informatics, The Hong Kong Polytechnic University, Kowloon, Hong Kong, China; [2]Department of Ultrasound, EDAN Instruments, Inc., Shenzhen, China; [3]Department of Ultrasound, Fifth Affiliated Hospital of Sun Yat-sen University, Zhuhai, China

Contributions: (I) Conception and design: Z Chen; (II) Administrative support: Z Su, MTC Ying; (III) Provision of study materials or patients: Z Chen, Z Su, MTC Ying; (IV) Collection and assembly of data: Z Chen, Y Wang, ST Gunda, X Han; (V) Data analysis and interpretation: Z Chen, Y Wang, ST Gunda, X Han; (VI) Manuscript writing: All authors; (VII) Final approval of manuscript: All authors.

Correspondence to: Ziman Chen, MD. Department of Health Technology and Informatics, The Hong Kong Polytechnic University, 11 Yuk Choi Rd, Hung Hom, Kowloon, Hong Kong 999077, China. Email: zimanchen@polyu.edu.hk; Zhongzhen Su, MD. Department of Ultrasound, Fifth Affiliated Hospital of Sun Yat-sen University, 52 Meihua East Rd, Zhuhai 519000, China. Email: sp9313@126.com; Michael Tin Cheung Ying, PhD. Department of Health Technology and Informatics, The Hong Kong Polytechnic University, 11 Yuk Choi Rd, Hung Hom, Kowloon, Hong Kong 999077, China. Email: michael.ying@polyu.edu.hk.

Background: Assessing renal fibrosis non-invasively in patients with chronic kidney disease (CKD) remains a considerable clinical challenge. This study aimed to investigate the diagnostic efficacy of different approaches that combine shear wave elastography (SWE) and estimated glomerular filtration rate (eGFR) in distinguishing between mild fibrosis and moderate-to-severe fibrosis in CKD patients.

Methods: In this prospective study, 162 patients underwent renal SWE examinations and renal biopsies. Using SWE, the right renal cortex stiffness was measured, and the corresponding SWE value was recorded. Four diagnostic patterns were used to combine eGFR and SWE value: in isolation, in series, in parallel, and in integration. The receiver operating characteristic (ROC) curve was established, and the area under the ROC curve (AUC) was calculated to quantify diagnostic performance. Sensitivity, specificity, and accuracy were computed.

Results: The eGFR demonstrated sensitivity of 68.2% and specificity of 83.8%, whereas the SWE value displayed sensitivity of 84.1% and specificity of 62.2%, yielding a similar AUC (78.2% and 77.8%, respectively). Combining in series improved specificity to 97.3%, superior to other diagnostic patterns (all P values <0.01), but compromised sensitivity to 58.0%. When combined in parallel, the sensitivity increased to 94.3%, exceeding any other strategies (all P values <0.05), but the specificity dropped to 48.7%. The integrated strategy, incorporating eGFR with SWE value via the logistic regression algorithm, exhibited an AUC of 85.8%, outperforming all existing approaches (all P values <0.01), with balanced sensitivity, specificity, and accuracy of 86.4%, 74.3%, and 80.9%, respectively.

Conclusions: Using an integrated strategy to combine eGFR and SWE value could improve diagnostic performance in distinguishing between mild renal fibrosis and moderate-to-severe renal fibrosis in patients with CKD, thereby helping clinicians perform a more accurate clinical diagnosis.

Keywords: Chronic kidney disease (CKD); renal fibrosis; shear wave elastography (SWE); estimated glomerular filtration rate (eGFR); diagnosis

Submitted Jul 01, 2023. Accepted for publication Nov 29, 2023. Published online Jan 02, 2024.
doi: 10.21037/qims-23-962
View this article at: https://dx.doi.org/10.21037/qims-23-962

Introduction

Globally, chronic kidney disease (CKD) is a growing health concern, with prevalence estimates indicating that approximately 9.1% of the population is affected (1,2). Progressive damage to the kidneys develops as a result of CKD, leading to a decline in kidney function and a host of potentially fatal complications, which ultimately require life-sustaining interventions such as kidney dialysis or transplantation (3,4). Renal fibrosis, which is marked by interstitial tissue damage, persistent inflammation, and excessive accumulation of extracellular matrix (ECM) components, is a pathological hallmark of CKD deteriorating to end-stage renal disease (ESRD) (5-7). Given these implications, it is imperative to undertake precise diagnostics and staging of renal fibrosis aiming at implementing efficacious intervention strategies to impede its progression.

Renal biopsy is considered the gold standard for evaluating renal fibrosis (8). However, this procedure is inherently intrusive and carries the potential for adverse complications, such as bleeding, infection, and arteriovenous fistulas (9,10). Additionally, the invasive nature of renal biopsies precludes repeated sampling in certain cases. Therefore, it is critical to develop alternative methods of assessing renal fibrosis that are less invasive and more cost-effective.

Shear wave elastography (SWE) is a state-of-the-art, non-invasive imaging modality that has been increasingly utilized in the clinical setting for a thorough examination of tissue stiffness (11,12). This innovative technique is predicated upon the fundamental principle of inducing shear waves within the tissue via the application of acoustic radiation force pulses (13). By measuring the propagation speed of shear waves or converting them into Young's modulus, tissue mechanical properties can be quantified. Several studies have revealed that SWE can provide valuable information regarding the differentiation of breast lesions (14), the diagnosis of thyroid nodules (15), and the detection of liver fibrosis (16). Previously, our research team also demonstrated the feasibility of applying SWE to assess renal fibrosis in CKD patients (17). Its diagnostic performance, however, does not meet desired clinical expectations, yielding an area under the curve (AUC) of 76.4% [95% confidence interval (CI): 68.1–84.8%]. In recent years, more and more researchers have set their sights on improving diagnosis strategies that combine ultrasound features with biomarker assays in a parallel or serial manner and have exhibited substantial promise in achieving satisfactory outcomes (18,19). These advancements in the field of medical diagnostics represent a significant development in the ongoing pursuit of effective and innovative healthcare solutions. However, whether SWE values combined with biomarker assays could enhance renal fibrosis diagnostic efficacy is still unclear.

Thus, in this study, we intend to evaluate the overall utility of these diagnostic patterns by combining SWE value with estimated glomerular filtration rate (eGFR), the primary indicator of renal function, via a variety of strategies, including (I) utilization of SWE value and eGFR in isolation; (II) combination in series; (III) combination in parallel; and (IV) combination in integration. To the best of our knowledge, this is the first study to investigate different diagnostic strategies using SWE value and a biomarker indicator for the assessment of renal fibrosis in patients with CKD. We present this article in accordance with the STARD reporting checklist (available at https://qims.amegroups.com/article/view/10.21037/qims-23-962/rc).

Methods

Study population

The present study was conducted in accordance with the Declaration of Helsinki (as revised in 2013). This study protocol was approved by the Ethics Committee of the Fifth Affiliated Hospital of Sun Yat-sen University (protocol code K09-1; approval date: May 2019). Informed written consent was obtained from all the subjects or their legal guardians. The study was prospectively conducted from April 2019 to December 2021, enrolling patients who attended the Department of Ultrasound at the Fifth Affiliated Hospital of Sun Yat-sen University. Patients presenting with CKD underwent a comprehensive assessment, including a renal biopsy, kidney function tests, and SWE examination. Pathological biopsies were performed by experienced clinicians following clinical diagnostic criteria. Likewise,

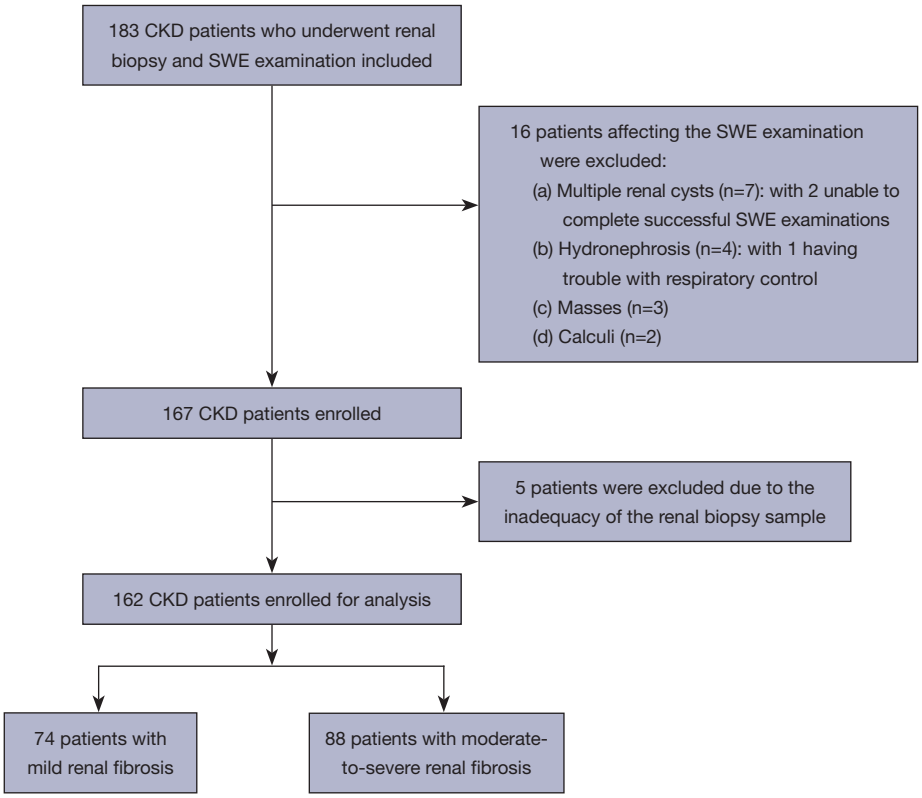

Figure 1 Flowchart of study population recruitment. CKD, chronic kidney disease; SWE, shear wave elastography.

kidney function assessments were conducted according to the patient's clinical care plan. SWE examination, a non-invasive and radiation-free procedure, presents no risk to patients. Prior to undertaking the SWE examination, a detailed explanation of the procedure was given to the patients or their legal guardians. The precise inclusion criteria were defined as follows: (I) the presence of CKD diagnosis, ascertained through the manifestation of renal impairment (evidenced by aberrations in blood or urine composition, renal biopsy findings, or radiological irregularities) or an enduring eGFR below 60 mL/min/1.73 m^2, consistently observed for over 3 months, in alignment with the 2012 Kidney Disease Improving Global Outcomes (KDIGO) guideline (20); (II) a prior eGFR assessment conducted before the renal biopsy; (III) a precedent SWE evaluation preceding the renal biopsy; (IV) a predetermined intention for renal fibrosis staging evaluation during the renal biopsy. The exclusion criteria for patients encompassed: (I) the presence of multiple renal cysts, calculi, hydronephrosis, or masses that could potentially interfere with the analysis conducted through SWE imaging; (II) the inability to adhere to prescribed respiratory control during the SWE procedure; (III) biopsy specimens deemed inadequate due to insufficient length (less than 10 mm) or fewer than 10 glomeruli; and (IV) unsuccessful SWE measurements. The workflow for patient selection is provided in *Figure 1*.

eGFR test

The eGFR was assessed within the week preceding the renal biopsy. In this study, the eGFR was calculated using the Chronic Kidney Disease Epidemiology Collaboration (CKD-EPI) formula (21). As per the 2012 KDIGO guidelines, eGFR accuracy was notably enhanced through employment of the CKD-EPI equation compared to the Modification of Diet in Renal Disease (MDRD) formula, especially for values exceeding 60 mL/min/1.73 m^2 (20). Moreover, the CKD-EPI equation finds preference in both general medical practice and public health contexts (22). In contrast, the Cockcroft-Gault equation tends to overestimate renal function, leading to decreased eGFR accuracy (23). Throughout the week preceding the eGFR assessment, the patients' initial treatment regimens remained relatively unchanged, or with only minor adjustments made when necessary. This

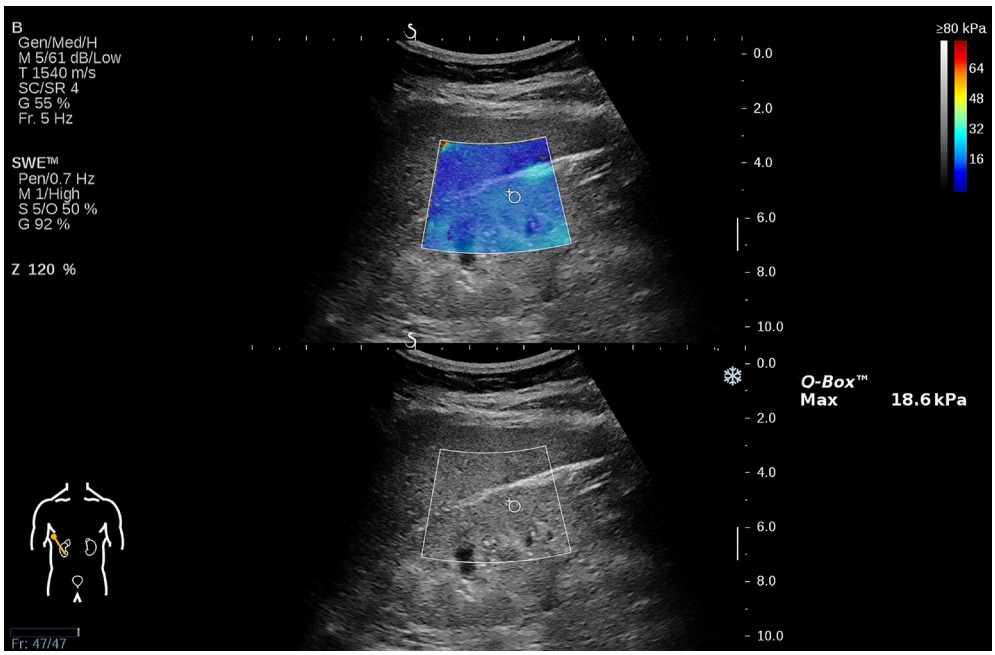

Figure 2 Use of a dual-modal display for shear wave elastography examination. The top image exhibits a color-coded elastogram for measuring renal stiffness, while the bottom image shows a grayscale B-mode image used for real-time elasticity imaging guidance.

precaution aimed to mitigate significant eGFR fluctuations linked to medication interventions.

SWE examination

A board-certified radiologist, possessing 6 years of specialized experience in abdominal ultrasound, conducted all SWE examinations two days prior to renal biopsy using the Aixplorer US imaging system (SuperSonic Imagine, Aix-en-Provence, France) equipped with the convex array probe (SC6-1, 1–6 MHz). Patients were required to void their bladders prior to the examination and maintain breath-holding for several seconds during the procedure. Under the guidance of B-mode ultrasound, the SWE procedure was performed in real-time to determine the elastic modulus of the cortex in the middle portion of the right kidney, with the patient in the supine position (*Figure 2*). To ensure precise inclusion of the renal cortex rather than the renal medulla in the renal elastography examination, a series of standardized procedures were employed. Initially, the elastography sampling frame (referred to as the Q-box) was minimized, with a fixed diameter of 4 mm. Subsequently, optimal placement of the Q-box was pursued by positioning it near the outer layer of the renal cortex, adjacent to the renal capsule, thereby circumventing the inclusion of the renal medulla. Furthermore, color Doppler ultrasound for assessing renal arcuate arteries was integrated into the protocol. This method proves advantageous in distinguishing between the renal cortex and the renal medulla. The resulting maximum SWE value, referred to as Emax, was recorded for each patient. According to our prior study, Emax, compared to other SWE parameters, demonstrated the greatest diagnostic performance in detecting renal fibrosis severity (17). Five independent and valid SWE measurements were obtained per patient and subjected to an arithmetic mean calculation for subsequent analysis. Since biopsy was only performed on the right renal parenchyma among the patient cohort, to achieve optimal congruence with the pathological assessment of renal fibrosis, only SWE parameters derived exclusively from the right kidney cortex were considered.

Renal biopsy

Indications for renal biopsy encompassed sustained proteinuria or hematuria and/or renal insufficiency. The ultrasound-guided renal biopsy was conducted at the lower pole of the right kidney, utilizing a 16- or 18-gauge automatic biopsy gun (Bard Magnum, Covington, GA, USA). Two experienced pathologists, each with 6 to 8 years'

experience, used light microscopy, immunofluorescence, and electron microscopy to evaluate the histopathology of renal biopsy specimens. Any discrepancies encountered were thoroughly discussed and resolved upon consensus. A comprehensive assessment of renal fibrosis was conducted through the use of a semi-quantitative scoring system. This evaluative approach was predicated upon pathological observations encompassing distinctive glomerular attributes (namely hypercellularity, segmental lesions, and global sclerosis), tubulointerstitial characteristics (including infiltration, fibrosis, and atrophy), as well as discernible vascular alterations (manifesting as wall thickening and hyaline changes). The formulation of this scoring scheme was previously expounded upon in our earlier investigation (17). The degree of fibrotic manifestation was ascertained through the classification of cases into three stratified cohorts predicated on their respective pathological scores: namely, mild (≤9 points), moderate (10–18 points), and severe (≥19 points). Due to the limited number of severe cases (n=18) in the present study, the moderate and severe cases were amalgamated into a single group for analysis, referred to as moderate-to-severe fibrosis.

Diagnosis strategy

Four distinct diagnosis strategies were established in the current study, as follows: (I) utilizing the SWE value and eGFR in isolation; (II) combining in series; (III) combining in parallel; and (IV) combining in integration. In the isolation strategy, either the SWE value or the eGFR was utilized as a standalone diagnostic variable to differentiate cases of mild renal fibrosis from those with moderate-to-severe fibrosis. This approach was designed to independently assess the diagnostic effectiveness of each individual variable. The serial strategy operated by identifying patients with moderate-to-severe fibrosis only when both the SWE value and the eGFR indicated the presence of such a condition. This method required dual confirmation from both diagnostic variables to categorize patients into the moderate-to-severe fibrosis group, emphasizing the importance of combined diagnostic evidence. In contrast to the serial approach, the parallel strategy identified patients with moderate-to-severe fibrosis if either the SWE value or the eGFR indicated this diagnosis. This strategy made use of the classification potential of the two diagnostic approaches and aimed to capture cases that might be missed by relying on a single parameter alone. The integration strategy leveraged a logistic regression algorithm to combine the SWE value and the eGFR, creating a unified approach. This method calculated the patient's risk probability of having moderate-to-severe fibrosis by incorporating both parameters. The diagnostic results were then determined based on a predefined cutoff value, which allowed for a reliable and accurate assessment.

Statistical analysis

All data analyses were conducted with SPSS 26.0 software (SPSS Inc., Chicago, IL, USA) and R statistical software (version 4.2.0; http://www.R-project.org). Continuous variables were expressed as either mean ± standard deviation or median (interquartile range), and their comparison was conducted utilizing either the Student's *t*-test or the Mann-Whitney *U* test. Categorical variables were presented as frequencies and compared with Pearson's Chi-squared test. The diagnostic variables were tested for normality through the Shapiro-Wilk normality test. An investigation of the association between diagnostic results and pathological findings was conducted using Pearson's Chi-squared test. By using Cohen's Kappa test, the degree of agreement between them was also determined. Accordingly, the agreement was classified as poor (0.00–0.20), fair (0.21–0.40), moderate (0.41–0.60), substantial (0.61–0.80), or almost flawless (0.81–1.00) (24,25). The receiver operating characteristic (ROC) curve was established, and the AUC was calculated to quantify the performance of the diagnostic patterns in differentiating between mild fibrosis and moderate-to-severe fibrosis. The Delong test was used to compare the AUCs of diagnostic approaches. The Youden index was determined by ROC analysis, and the maximum tangent point was identified to obtain the optimal cutoff value of the diagnostic patterns. The corresponding sensitivity, specificity, and accuracy were also computed. Sensitivities and specificities of paired diagnostic strategies were compared using the McNemar test. Comparison of accuracies between diagnostic strategies was performed by Pearson's Chi-squared test. Statistical significance was defined as a two-sided $P<0.05$.

Results

Baseline characteristics of study population

Twenty-one subjects were excluded from the study due to non-compliance with selection criteria. Specifically, these

Table 1 Baseline characteristics of participants

Characteristic	All (n=162)	Mild (n=74)	Moderate-to-severe (n=88)	P value
Gender (male/female)	91/71	43/31	48/40	0.649
Age (years)	40.41±14.26, [16–74]	34.47±12.89, [16–67]	45.40±13.48, [16–74]	<0.001
eGFR (mL/min/1.73 m^2)	89.43 (55.89–113.21), [4.41–147.86]	108.14 (89.82–121.24), [16.50–147.86]	63.32 (41.35–96.30), [4.41–139.00]	<0.001
SWE value (kPa)	34.38±9.90, [13.16–59.04]	39.62±9.25, [20.20–59.04]	29.96±8.14, [13.16–49.20]	<0.001
Etiology				–
IgA nephropathy	72	27	45	
Membranous nephropathy	34	16	18	
MCN	16	16	0	
MsPGN	9	4	5	
Lupus nephritis	9	5	4	
FSGS	8	3	5	
Diabetic nephropathy	6	0	6	
Others	5	2	3	
Unknowns	3	1	2	

Categorical variables are presented as number and continuous variables as mean ± standard deviation [range] or median (interquartile range) [range], as appropriate. The P value is calculated based on the comparison between the mild and moderate-to-severe groups. eGFR, estimated glomerular filtration rate; SWE, shear wave elastography; MCN, minimal change nephropathy; MsPGN, mesangial proliferative glomerulonephritis; FSGS, focal segmental glomerular sclerosis.

exclusions were attributed to the presence of multiple renal cysts (n=7), masses (n=3), hydronephrosis (n=4), calculi (n=2), as well as the inadequacy of renal biopsy samples (n=5). Notably, within this subject cohort, two individuals with multiple renal cysts were precluded from successful SWE assessments. Furthermore, in hydronephrosis cases, one subject encountered difficulty in maintaining appropriate respiratory control during the diagnostic evaluation. Finally, 162 patients were included in this study, of whom 74 (45.7%) had biopsy-proven mild renal fibrosis and 88 (54.3%) had moderate-to-severe renal fibrosis. The eGFR was 89.43 (interquartile range, 55.89–113.21) mL/min/1.73 m^2 in the study cohort, while the SWE value was 34.38±9.90 kPa. The SWE values followed a normal distribution (P value =0.384), whereas the eGFR values were not normally distributed (P value <0.01) (Figures S1,S2). The baseline characteristics are summarized in *Table 1*.

Diagnostic consistency with pathological findings

All diagnostic approaches were statistically significant in identifying moderate-to-severe from mild renal fibrosis (all P values <0.001). The diagnostic results were moderately consistent with pathological findings for eGFR (Kappa =0.511), SWE (Kappa =0.470), serial scheme (Kappa =0.532), and parallel scheme (Kappa =0.445), whereas the integrated scheme (Kappa =0.611) had substantial agreement (*Table 2*).

Performance of different diagnostic strategies

An optimal cutoff value was determined according to the Youden index, wherein the eGFR was set at 84.10 mL/min/1.73 m^2 and the SWE value was 37.14 kPa (*Figure 3*). Within the integrated strategy, in accordance with the logistic regression algorithm, the diagnostic formula was as follows: Diagnostic probability = 7.23 – 0.03 × eGFR – 0.12 × SWE value. Utilizing the Youden index, the optimal threshold value for diagnostic probability was established at –0.19.

In the isolated strategy, the eGFR achieved a sensitivity of 68.2% (95% CI: 57.3–77.5%) and a specificity of 83.8% (95% CI: 73.0–91.0%) in identifying patients with moderate-to-severe renal fibrosis from mild ones, while the SWE value yielded a sensitivity of 84.1% (95% CI: 74.4–

Table 2 Consistency analysis between diagnostic patterns and pathological results

Index	Subtypes	Pathological result		Cohen's Kappa value (95% CI)	χ^2	P value
		Mild	Moderate-to-severe			
eGFR	Mild	62	28	0.511 (0.382–0.640)	43.936	<0.001
	Moderate-to-severe	12	60			
SWE	Mild	46	14	0.470 (0.334–0.605)	36.877	<0.001
	Moderate-to-severe	28	74			
Serial scheme	Mild	72	37	0.532 (0.416–0.649)	55.747	<0.001
	Moderate-to-severe	2	51			
Parallel scheme	Mild	36	5	0.445 (0.318–0.573)	39.258	<0.001
	Moderate-to-severe	38	83			
Integrated scheme	Mild	55	12	0.611 (0.489–0.734)[&]	61.043	<0.001
	Moderate-to-severe	19	76			

[&], the value indicates the highest diagnostic performance in this metric. CI, confidence interval; eGFR, estimated glomerular filtration rate; SWE, shear wave elastography.

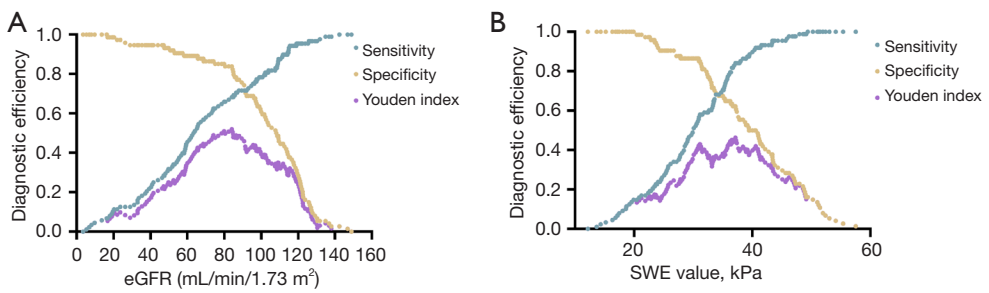

Figure 3 Scatter plots illustrating the trend of diagnostic metric changes for eGFR and SWE value in relation to the Youden index variation. eGFR, estimated glomerular filtration rate; SWE, shear wave elastography.

90.7%) and a specificity of 62.2% (95% CI: 50.1–73.0%). These two diagnostic patterns attained a similar AUC of 78.2% (95% CI: 70.9–85.4%) for eGFR and 77.8% (95% CI: 70.6–85.0%) for SWE, respectively. Combining the eGFR and SWE value in series improved the specificity of the classification results to 97.3% (95% CI: 89.7–99.5%), outperforming other diagnostic patterns (all P values <0.01), at the cost of a compromise in sensitivity to 58.0% (95% CI: 47.0–68.2%). The yielding AUC was still maintained at 77.6% (95% CI: 72.1–83.1%). When the eGFR was combined with the SWE value in parallel, the diagnosis approach achieved a sensitivity of 94.3% (95% CI: 86.6–97.9%), exceeding any other strategies (all P values <0.05), but the specificity dropped to 48.7% (95% CI: 37.0–60.5%), accompanied by a slightly decreased AUC of 71.5% (95% CI: 65.3–77.7%). Concerning the integrated strategy, in which the eGFR was incorporated with the SWE value via the logistic regression algorithm, both sensitivity and specificity exhibited satisfactory performance, with values of 86.4% (95% CI: 77.0–92.5%) and 74.3% (95% CI: 62.6–83.5%), respectively, for efficiency. In addition, the AUC (85.8%; 95% CI: 80.0–91.6%), derived from the integrated approach, was superior to all other approaches (DeLong test, all P values <0.01) (*Figure 4*). The integrated approach achieved the highest accuracy (80.9%; 95% CI: 73.8–86.4%); however, the difference was not significant when compared to the other diagnostic schemes (all P values >0.05), except for the parallel approach (P=0.029).

The performance of all the diagnosis strategies is detailed in *Table 3*.

Deployment of auxiliary diagnostic device

Given that the diagnostic performance of the integrated strategy was relatively comprehensive, it was deemed the most appropriate diagnostic approach for this medical issue. As part of this study, an easy-to-use document-based diagnostic tool (Appendix 1) derived from the integrated strategy was developed to facilitate real-life applications. The ability to enter eGFR and SWE value on the document page is a very helpful way for clinicians to make a diagnosis.

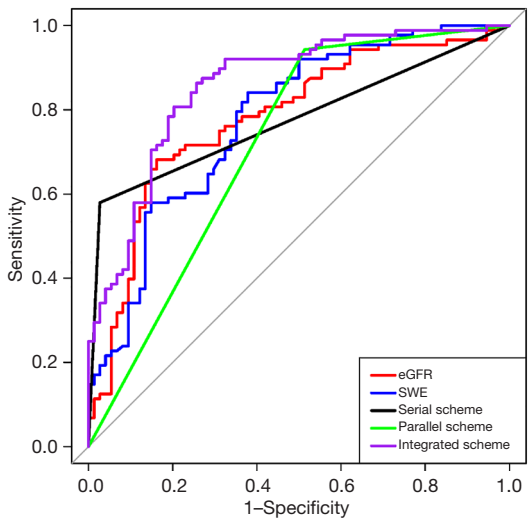

Figure 4 Comparison of receiver operating characteristic curves for each diagnostic strategy. eGFR, estimated glomerular filtration rate; SWE, shear wave elastography.

Discussion

The present study endeavors to optimize the diagnostic efficacy of readily accessible diagnostic variables by devising diverse diagnostic strategies. A combination of eGFR and SWE value in a series could enhance clinical capability for distinguishing patients with mild renal fibrosis. For the identification of patients with moderate-to-severe renal fibrosis, the parallel combination of eGFR and SWE value is beneficial. It is critical to note that both of these diagnostic strategies have a trade-off; that is, if sensitivity is improved, a price must be paid for reduced specificity, and vice versa (26). Moreover, diagnosis accuracy has not improved significantly, and in the parallel approach, it was even inferior to the diagnostic variables when used alone. The integrated strategy significantly ameliorated the above phenomenon. In contrast, there was a significant improvement in diagnosis performance with the integrated approach, which outperformed all other diagnostic strategies and had satisfactory sensitivity and specificity. Utilizing a simple combination approach, the integrated strategy could maximize the analytical information of variables within existing resources, enhancing and optimizing diagnosis power, and thereby supporting clinical decision-making (27). To enhance clinical utility, we have developed an offline, document-based diagnostic device founded on the integrated strategy. This tool enables the immediate derivation of patients' diagnostic outcomes through the straightforward input of essential diagnostic variables. Notably, the diagnostic device relies on laboratory

Table 3 Comparison of diagnostic performance between various approaches

Index	AUC		Sensitivity		Specificity		Accuracy	
	% (95% CI)	P value	% (95% CI)	P value#	% (95% CI)	P value*	% (95% CI)	P value^
eGFR	78.2 (70.9–85.4)	0.006	68.2 (57.3–77.5)	<0.001	83.8 (73.0–91.0)	0.002	75.3 (67.8–81.6)	0.175
SWE	77.8 (70.6–85.0)	0.005	84.1 (74.4–90.7)	0.004	62.2 (50.1–73.0)	<0.001	74.1 (66.5–80.5)	0.080
Serial scheme	77.6 (72.1–83.1)	0.006	58.0 (47.0–68.2)	<0.001	97.3 (89.7–99.5)[&]	–	75.9 (68.5–82.1)	0.280
Parallel scheme	71.5 (65.3–77.7)	<0.001	94.3 (86.6–97.9)[&]	–	48.7 (37.0–60.5)	<0.001	73.5 (65.9–79.9)	0.029
Integrated scheme	85.8 (80.0–91.6)[&]	–	86.4 (77.0–92.5)	0.016	74.3 (62.6–83.5)	<0.001	80.9 (73.8–86.4)[&]	–

P value refers to comparing with an integrated scheme; P value# refers to comparing with a parallel scheme; P value* refers to comparing with a serial scheme; and P value^ refers to comparing with an integrated scheme. [&], the value indicates the highest diagnostic performance in this metric. AUC, area under the curve; CI, confidence interval; eGFR, estimated glomerular filtration rate; SWE, shear wave elastography.

tests and imaging parameters derived from individuals diagnosed with CKD, rendering it being exclusively applicable to this patient cohort. For the general population, the absence of invasive kidney biopsies precludes access to kidney pathology data, thereby rendering it unsuitable for the development of diagnostic tools targeting this demographic.

Due to inherent renal anisotropy, a notable disparity in elastic measurements was observed between the renal poles and the mid-region. This distinction arises from the insonation angle formed by the ultrasound beam and the cortical surface (28). The coefficients of variation for elastic measurements in the mid-region (10.2%) exhibited a considerably weaker value than the lower pole (16.4%) ($P<0.05$) (29). Additionally, the rate of successful measurements at the renal poles was comparatively lower than those taken in the central segment of the renal parenchyma. This observation underscores the recommendation to exclude the renal poles from measurements, a practice that enhances measurement reproducibility (30). As a result, elastic imaging measurements were specifically conducted in the central region of the kidney. To mitigate the risk of substantial post-puncture bleeding caused by inadvertent damage to major blood vessels, renal biopsies are ideally conducted at the lower pole of the kidney. However, in the context of diffuse renal parenchymal lesions, no disparities were observed in the extent of renal fibrosis as assessed across various renal biopsy sites. The dimensions of the biopsy core, the glomerular count per core, and the indicators of chronic renal damage (including the extent of interstitial fibrosis and the proportion of globally or segmentally scarred glomeruli) remained unaffected by the biopsy site (whether located at the pole or mid-portion) (31). Additionally, no statistically significant disparity was noted in the arterial count between biopsies acquired from the two distinct biopsy regions. Hence, even when the renal biopsy site is situated at the lower pole of the kidney, the degree of renal fibrosis assessed through this approach remains representative and effectively mirrors the fibrotic status within the kidney's central region (32).

In a recent investigation, Ge *et al.* introduced a radiomics nomogram that incorporates radiomics scores from SWE images with independently predictive clinical factors (33). The study demonstrated promising results in differentiating renal fibrosis severity among CKD patients, yielding an AUC ranging from 0.83 to 0.85—results comparable to our proposed diagnostic approach. However, the practical implementation of the radiomics nomogram necessitates an initial delineation of the region of interest within the SWE image, followed by the utilization of specialized computer software to extract radiomics features and produce radiomics labels. This complex procedure inevitably increases medical practitioners' workload. Moreover, the process requires the availability of specialized radiomics analysis software, a resource often absent from numerous clinical departments. Additionally, the biological interpretation of radiomics remains an unresolved matter that requires additional investigation (34). Consequently, this dearth significantly compromises clinical implementation. In marked contrast, the diagnostic tool derived from our research distinguishes itself through its simplicity and user-friendliness. A straightforward input of variables into the document is sufficient for the immediate generation of the degree of kidney fibrosis—either categorized as mild or indicative of progressing to moderate-to-severe fibrosis.

In the context of an isolated diagnostic strategy, which relies solely on the eGFR value to distinguish between mild and moderate-to-severe renal fibrosis in CKD patients, a specific eGFR threshold of 84.10 mL/min/1.73 m^2 was determined using the Youden index. The diagnostic outcomes obtained from this approach demonstrated its ability to accurately identify a substantial portion of CKD patients with mild renal fibrosis (62/74). However, it also resulted in an erroneous classification of a significant number of patients with moderate-to-severe renal fibrosis as belonging to mild renal fibrosis (28/88). In this particular isolated diagnostic method, the eGFR threshold derived from the Youden index was found to be somewhat elevated, which may be related to the CKD diagnostic criteria. It is worth noting that there are two primary diagnostic criteria for CKD (20). The first criterion defines CKD when hematuria, urine protein, kidney biopsy pathological findings, or imaging indicators of kidney structural damage are abnormal for a duration exceeding three months, regardless of the level of eGFR impairment. The second criterion diagnoses CKD if the eGFR remains below 60 mL/min/1.73 m^2 for more than three months, irrespective of the status of other kidney-related indicators. While eGFR is a commonly used laboratory measure for assessing renal function in clinical practice, these diagnostic criteria emphasize that it is not the sole determinant. The higher eGFR threshold resulting from the Youden index calculation may be influenced by additional factors inherent to the diagnostic criteria, potentially contributing to the limited diagnostic capability when employing the eGFR

indicator in isolation as a diagnostic strategy. This also underscores the need for a combined diagnostic strategy.

In the present study, the eGFR in this study cohort measured 89.43 (interquartile range, 55.89–113.21) mL/min/1.73 m^2. Notably, a prior study reported eGFR values for CKD patients with fibrosis at 48.02±33.70 mL/min/1.73 m^2 (33). It is critical to note that the previous study exclusively employed eGFR as the sole diagnostic criterion for CKD, necessitating eGFR values below 60 mL/min/1.73 m^2 for diagnosis. Consequently, the eGFR values of the subjects included in that study were significantly lower than those in this investigation. However, it is imperative to emphasize that, in line with the KDIGO 2012 diagnostic criteria for CKD, as delineated above, eGFR does not stand as the sole diagnostic criterion (20). Therefore, the inclusion criteria for CKD cases in the prior study appeared to lack precision and rationale. This difference accounts for the significant variation observed in eGFR values between this study and previous research. Additionally, a study by Islamoglu *et al.* reported an eGFR value of 87.33±40.17 mL/min/1.73 m^2 in CKD patients with renal fibrosis, which aligns with our own research findings (35).

Even though some advancements have been made in this study, there are still some limitations. First, it is noteworthy that the cohort of eligible participants within the severe renal fibrosis group was of a limited size. Consistent with epidemiological reports, the prevalence rates for CKD stages 1–2, stage 3, stage 4, and stage 5 are documented as 5.0%, 3.9%, 0.16%, and 0.07%, respectively (1). Hence, there arises a necessity to substantiate these findings through a broader sample size, underscoring the imperative of validation on a larger scale. Second, our results were derived from a single-center setting, and the main findings need to be further validated at the multicenter level. Third, the present study did not evaluate the cost-effectiveness of deploying the suggested integrated strategy in clinical practice. This aspect bears the potential for further investigation in real-world clinical settings.

Conclusions

Our study demonstrated that the combination of eGFR and SWE value via an integrated strategy could improve diagnostic performance in distinguishing between mild renal fibrosis and moderate-to-severe renal fibrosis in patients with CKD. This strategy would help clinicians perform a more accurate clinical diagnosis in this clinical context.

Acknowledgments

Funding: None.

Footnote

Reporting Checklist: The authors have completed the STARD reporting checklist. Available at https://qims.amegroups.com/article/view/10.21037/qims-23-962/rc

Conflicts of Interest: All authors have completed the ICMJE uniform disclosure form (available at https://qims.amegroups.com/article/view/10.21037/qims-23-962/coif). Y.W. is affiliated with EDAN Instruments, Inc. The other authors have no conflicts of interest to declare.

Ethical Statement: The authors are accountable for all aspects of the work in ensuring that questions related to the accuracy or integrity of any part of the work are appropriately investigated and resolved. This study protocol was approved by the Ethics Committee of the Fifth Affiliated Hospital of Sun Yat-sen University (protocol code K09-1; approval date: May 2019) and conducted in accordance with the Declaration of Helsinki (as revised in 2013). Written informed consent to participate was obtained from all subjects themselves or their legal guardians.

References

1. GBD Chronic Kidney Disease Collaboration. Global, regional, and national burden of chronic kidney disease, 1990-2017: a systematic analysis for the Global Burden of Disease Study 2017. Lancet 2020;395:709-33.
2. Yang C, Gao B, Zhao X, Su Z, Sun X, Wang HY, et al. Executive summary for China Kidney Disease Network (CK-NET) 2016 Annual Data Report. Kidney Int 2020;98:1419-23.
3. Zhang L, Zhao MH, Zuo L, Wang Y, Yu F, Zhang H,

Wang H; CK-NET Work Group. China Kidney Disease Network (CK-NET) 2016 Annual Data Report. Kidney Int Suppl (2011) 2020;10:e97-e185.
4. Legrand K, Speyer E, Stengel B, Frimat L, Ngueyon Sime W, Massy ZA, Fouque D, Laville M, Combe C, Jacquelinet C, Durand AC, Edet S, Gentile S, Briançon S, Ayav C. Perceived Health and Quality of Life in Patients With CKD, Including Those With Kidney Failure: Findings From National Surveys in France. Am J Kidney Dis 2020;75:868-78.
5. Panizo S, Martínez-Arias L, Alonso-Montes C, Cannata P, Martín-Carro B, Fernández-Martín JL, Naves-Díaz M, Carrillo-López N, Cannata-Andía JB. Fibrosis in Chronic Kidney Disease: Pathogenesis and Consequences. Int J Mol Sci 2021;22:408.
6. Humphreys BD. Mechanisms of Renal Fibrosis. Annu Rev Physiol 2018;80:309-26.
7. Hou FF, Liu Y. New insights into the pathogenesis and therapeutics of kidney fibrosis. Kidney Int Suppl (2011) 2014;4:1.
8. Hogan JJ, Mocanu M, Berns JS. The Native Kidney Biopsy: Update and Evidence for Best Practice. Clin J Am Soc Nephrol 2016;11:354-62.
9. Halimi JM, Gatault P, Longuet H, Barbet C, Bisson A, Sautenet B, Herbert J, Buchler M, Grammatico-Guillon L, Fauchier L. Major Bleeding and Risk of Death after Percutaneous Native Kidney Biopsies: A French Nationwide Cohort Study. Clin J Am Soc Nephrol 2020;15:1587-94.
10. Trajceska L, Severova-Andreevska G, Dzekova-Vidimliski P, Nikolov I, Selim G, Spasovski G, Rambabova-Busletik I, Ristovska V, Grcevska L, Sikole A. Complications and Risks of Percutaneous Renal Biopsy. Open Access Maced J Med Sci 2019;7:992-5.
11. Cosgrove D, Piscaglia F, Bamber J, Bojunga J, Correas JM, Gilja OH, et al. EFSUMB guidelines and recommendations on the clinical use of ultrasound elastography. Part 2: Clinical applications. Ultraschall Med 2013;34:238-53.
12. Cao H, Ke B, Lin F, Xue Y, Fang X. Shear Wave Elastography for Assessment of Biopsy-Proven Renal Fibrosis: A Systematic Review and Meta-analysis. Ultrasound Med Biol 2023;49:1037-48.
13. Bamber J, Cosgrove D, Dietrich CF, Fromageau J, Bojunga J, Calliada F, et al. EFSUMB guidelines and recommendations on the clinical use of ultrasound elastography. Part 1: Basic principles and technology. Ultraschall Med 2013;34:169-84.
14. Barr RG, Nakashima K, Amy D, Cosgrove D, Farrokh A, Schafer F, et al. WFUMB guidelines and recommendations for clinical use of ultrasound elastography: Part 2: breast. Ultrasound Med Biol 2015;41:1148-60.
15. Cosgrove D, Barr R, Bojunga J, Cantisani V, Chammas MC, Dighe M, Vinayak S, Xu JM, Dietrich CF. WFUMB Guidelines and Recommendations on the Clinical Use of Ultrasound Elastography: Part 4. Thyroid. Ultrasound Med Biol 2017;43:4-26.
16. Ferraioli G, Filice C, Castera L, Choi BI, Sporea I, Wilson SR, et al. WFUMB guidelines and recommendations for clinical use of ultrasound elastography: Part 3: liver. Ultrasound Med Biol 2015;41:1161-79.
17. Chen Z, Chen J, Chen H, Su Z. Evaluation of renal fibrosis in patients with chronic kidney disease by shear wave elastography: a comparative analysis with pathological findings. Abdom Radiol (NY) 2022;47:738-45.
18. Velayo CL, Reforma KN, Sicam RVG, Diwa MH, Sy ADR, Tantengco OAG. Improving diagnostic strategies for ovarian cancer in Filipino women using ultrasound imaging and a multivariate index assay. Cancer Epidemiol 2022;81:102253.
19. Duan X, Peng Y, Liu W, Yang L, Zhang J. Does Supersonic Shear Wave Elastography Help Differentiate Biliary Atresia from Other Causes of Cholestatic Hepatitis in Infants Less than 90 Days Old? Compared with Grey-Scale US. Biomed Res Int 2019;2019:9036362.
20. Stevens PE, Levin A; Kidney Disease: Improving Global Outcomes Chronic Kidney Disease Guideline Development Work Group Members. Evaluation and management of chronic kidney disease: synopsis of the kidney disease: improving global outcomes 2012 clinical practice guideline. Ann Intern Med 2013;158:825-30.
21. Inker LA, Schmid CH, Tighiouart H, Eckfeldt JH, Feldman HI, Greene T, Kusek JW, Manzi J, Van Lente F, Zhang YL, Coresh J, Levey AS; CKD-EPI Investigators. Estimating glomerular filtration rate from serum creatinine and cystatin C. N Engl J Med 2012;367:20-9.
22. Earley A, Miskulin D, Lamb EJ, Levey AS, Uhlig K. Estimating equations for glomerular filtration rate in the era of creatinine standardization: a systematic review. Ann Intern Med 2012;156:785-95.
23. Schwandt A, Denkinger M, Fasching P, Pfeifer M, Wagner C, Weiland J, Zeyfang A, Holl RW. Comparison of MDRD, CKD-EPI, and Cockcroft-Gault equation in relation to measured glomerular filtration rate among a large cohort with diabetes. J Diabetes Complications 2017;31:1376-83.

24. Viera AJ, Garrett JM. Understanding interobserver agreement: the kappa statistic. Fam Med 2005;37:360-3.
25. Landis JR, Koch GG. The measurement of observer agreement for categorical data. Biometrics 1977;33:159-74.
26. Schlattmann P. Statistics in diagnostic medicine. Clin Chem Lab Med 2022;60:801-7.
27. Harrell FE. Regression modeling strategies. Bios 2017;330:14.
28. Liu X, Li N, Xu T, Sun F, Li R, Gao Q, Chen L, Wen C. Effect of renal perfusion and structural heterogeneity on shear wave elastography of the kidney: an in vivo and ex vivo study. BMC Nephrol 2017;18:265.
29. Lin Y, Chen J, Huang Y, Lin Y, Su Z. A methodological study of 2D shear wave elastography for noninvasive quantitative assessment of renal fibrosis in patients with chronic kidney disease. Abdom Radiol (NY) 2023;48:987-98.
30. Bob F, Bota S, Sporea I, Sirli R, Petrica L, Schiller A. Kidney shear wave speed values in subjects with and without renal pathology and inter-operator reproducibility of acoustic radiation force impulse elastography (ARFI)--preliminary results. PLoS One 2014;9:e113761.
31. Peters B, Mölne J, Hadimeri H, Hadimeri U, Stegmayr B. Sixteen Gauge biopsy needles are better and safer than 18 Gauge in native and transplant kidney biopsies. Acta Radiol 2017;58:240-8.
32. Gerth J, Busch M, Illner N, Traut M, Gröne HJ, Wolf G. Are tissue samples from two different anatomical areas of the kidney necessary for adequate diagnosis? Clin Nephrol 2010;74:258-65.
33. Ge XY, Lan ZK, Lan QQ, Lin HS, Wang GD, Chen J. Diagnostic accuracy of ultrasound-based multimodal radiomics modeling for fibrosis detection in chronic kidney disease. Eur Radiol 2023;33:2386-98.
34. Fournier L, Costaridou L, Bidaut L, Michoux N, Lecouvet FE, de Geus-Oei LF, et al. Incorporating radiomics into clinical trials: expert consensus endorsed by the European Society of Radiology on considerations for data-driven compared to biologically driven quantitative biomarkers. Eur Radiol 2021;31:6001-12.
35. Islamoglu MS, Gulcicek S, Seyahi N. Kidney tissue elastography and interstitial fibrosis observed in kidney biopsy. Ren Fail 2022;44:314-9.

Cite this article as: Chen Z, Wang Y, Gunda ST, Han X, Su Z, Ying MTC. Integrating shear wave elastography and estimated glomerular filtration rate to enhance diagnostic strategy for renal fibrosis assessment in chronic kidney disease. Quant Imaging Med Surg 2024;14(2):1766-1777. doi: 10.21037/qims-23-962

Supplementary

Appendix 1

Severity of Renal Fibrosis - Integrated Strategy			
Predictors	Units	Case value	Note
eGFR	ml/min/1.73 m^2	100	
SWE value	kPa	50	
The Diagnosis is	Mild Renal Fibrosis		

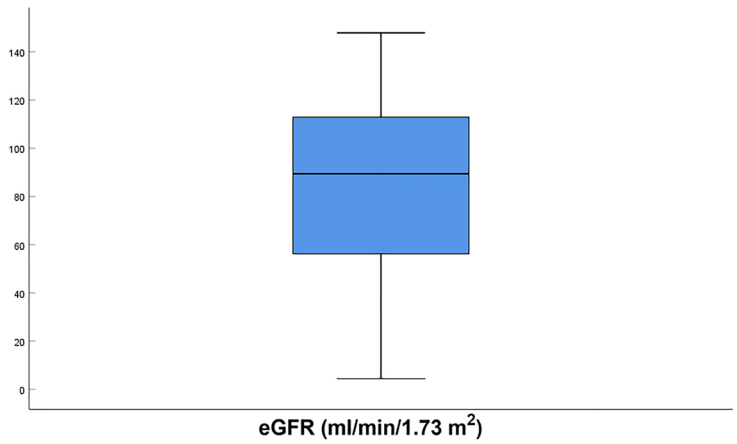

Figure S1 Box plot of eGFR. eGFR, estimated glomerular filtration rate.

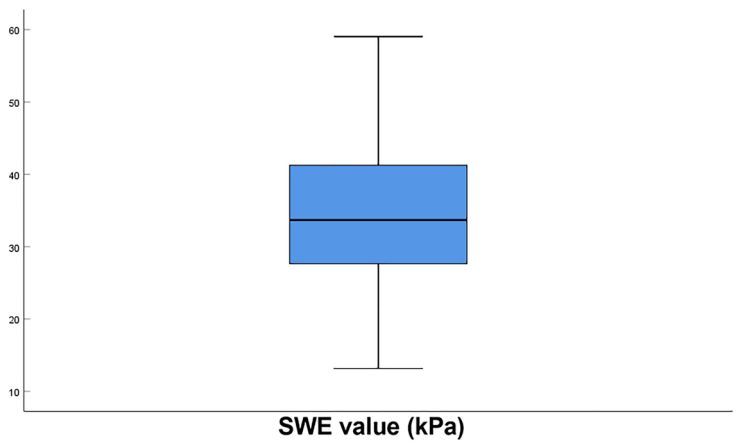

Figure S2 Box plot of SWE value. SWE, shear wave elastography.

https://dx.doi.org/10.21037/qims-23-962